EFFECTS OF HETEROGENEITY OF MICROCRYSTALLINE CELLULOSE WITH NANO-SiO_2 ON ITS APPLICATION IN TIRE TREAD COMPOUNDS

YU DU, YUEQIAO WU, XIAOFAN MA, YUNHAO HU, HONGHUA BI and JUTAO SUN

Key Laboratory of Rubber-Plastics, Ministry of Education, Shandong Provincial Key Laboratory of Rubber-Plastics, Qingdao University of Science and Technology, PO Box 73, Qingdao, 266042, People's Republic of China

✉ *Corresponding author: Jutao Sun, sjt-hit@163.com*

Received July 27, 2019

Heterostructures of microcrystalline cellulose-SiO_2 nanoparticles (MCC-SiO_2) were prepared by adsorption phase reaction technology (APRT). A urea solution served as the adsorption phase in the swelling process of the MCC particles. The thickness of the urea solution layer that adsorbed on the MCC surface was controlled by washing the samples with ethanol 3 times. The urea layer acted as a "microreactor" to generate SiO_2 nanoparticles through a sol-gel process with tetraethoxysilane (TEOS), and MCC-SiO_2 heterostructures took shape. The morphologies of the heterostructures were controllable by changing the swelling time, thickness of the urea layer and TEOS content. The SiO_2 particles loaded on the MCC surface were almost spherical, with a size of 20-40 nm. These heterostructures were used in tire tread compounds to show their potential as reinforcing fillers. Compared with vulcanizates filled with MCC, those filled with the heterostructures had improved mechanical properties, with a 16.7% increase in tensile strength and a 16.2% increase in tear strength. Furthermore, the heterostructures were found to be a good filler for addressing the "magic triangle" problem in the tire industry. These materials improved the wet-skid resistance and abrasion resistance, and decreased the rolling resistance. These results indicated that MCC-SiO_2 heterostructures are a potential filler for use in the tire industry. SEM photographs showed that the sizes of the MCC-SiO_2 heterostructures were micronized *in situ* during rubber processing, from 20-90 μm to 1-10 μm, and the interfacial bonding between the heterostructures and the rubber matrix was improved.

Keywords: microcrystalline cellulose, nano-SiO_2, heterostructures, wet-skid resistance, tire tread compounds

INTRODUCTION

Currently, there is a trend of developing environmentally friendly materials, renewable resources and energy, and sustainable techniques to ease the burden of nonbiodegradable petroleum-based materials and meet the demand for environmental protection and resource conservation.[1,2] Natural polymers have received increasing amounts of attention in the development of environmentally friendly, biocompatible and biodegradable products.[3,4] Among these materials, cellulose-based materials are the most attractive due to their renewability, biocompatibility, biodegradability, availability, nontoxicity and low cost.[5,6] Microcrystalline cellulose (MCC) can be prepared from raw cellulose through simple physical methods, such as mechanical disintegration, steam explosion, and chemical methods, such as acid hydrolysis and enzymolysis.[7-11] MCC is a commercially available product with high crystallinity and strength, but larger sizes (20-90 μm). MCC can be further treated by acid hydrolysis to prepare nanocrystalline cellulose (NCC), rod-like, with 3-5 nm width and 50-500 nm in length.[2,12,13] In recent years, there has been an attempt to use MCC and NCC as "green fillers" in plastic and rubber composites.[14-18]

NCC has satisfactory reinforcing efficiency due to being nano-sized and having high strength, but it is not easily available because of production difficulties and high price. Furthermore, it is difficult to disperse NCC in a

rubber matrix because of its strong tendency to aggregate, which seriously limits its application in polymer composites. MCC is commercially available, but its use is restricted by its poor reinforcing efficiency resulting from its large size (20-90 μm) and poor compatibility with nonpolar rubber. Many attempts have been made to solve these two problems, such as chemical grafting, esterification and silanization.[19-22] These chemical methods can improve its compatibility with a polymer matrix, but have little benefit in decreasing the size of MCC. The high cost and complicated process have limited the large-scale application of MCC.

The adsorption phase reaction technique (APRT) is a new microreactor technique to prepare nanocomposites and nanocomposite catalysts, usually using silicate or SiO_2 particles as a nanoparticle carrier.[23] MCC has a strong hydrophilicity and is capable of absorbing a thin water layer to serve as a microreactor where inorganic particles can be generated and loaded on its surface. In our previous work, it was found that rod-like, tube-like and spherical SiO_2 or ZnO particles could be loaded on the surface of MCC (swollen by 8% NaOH solution) by the APRT method.[24-26] Further studies showed that the crystal form of MCC changed after being swollen by NaOH solution, which decreased the reinforcement in rubber compounds. The rod-like and tube-like SiO_2 or ZnO particles were not helpful in reinforcement because their shapes were destroyed under the force field during rubber processing. In this paper, a urea aqueous solution was used as swelling agent for MCC to avoid the destruction of MCC crystallinity and to control the shapes of nano-SiO_2 particles that were generated on the surface of MCC. The MCC-SiO_2 heterostructures were then used in tire tread compounds, and their effects on the mechanical properties, wet-skid resistance, rolling resistance and abrasion resistance of the tread compounds were investigated.

EXPERIMENTAL

Materials

Microcrystalline cellulose (20-90 μm in length and 5-20 μm in width) was supplied by Shandong Liaocheng Luxi Medicinal Materials Co., Ltd., China. The urea, ammonium hydroxide ($NH_3.H_2O$, NH_3 content was 25 wt%), alcohol, and tetraethoxysilane (TEOS), analytically pure, were all purchased from National Pharmaceutical Group Chemical Reagent Co., Ltd., China. The ingredients of the tire tread compounds are listed in Table 1. The elastomers were solution-polymerized styrene butadiene rubber (SSBR2557A, the styrene content was approximately 25%, and butadiene content was approximately 75%), and the emulsion-polymerized styrene butadiene rubber (ESBR1502, the styrene content was approximately 23.5%, and the butadiene content was approximately 76.5%) was supplied by Sinopec Dushanzi Co. Ltd., China. The silica (1165 MP, with a specific surface area of 165 m^2/g) was obtained from Solvay Fine Chemical Additives Qingdao Co., Ltd., China. N-1,3-dimethylbutyl-N'-phenyl-p-phenylenediamine (antioxidant 4020) and poly(1,2-dihydro-2,2,4-trimethyl-quinoline) (antioxidant RD) were received from Shanghai Chengjin Chemicals Co., Ltd., China. The other ingredients, including [3-(triethoxysilyl)propyl]tetrasulfide (Si69), diphenylguanidine (DPG), sulfur, stearic acid (SA), N-tertiarybutyl-2-benzothiazole sulfonamide (TBBS), zinc oxide (ZnO) and wax, industrial grade, were supplied by Sentury Tires Co., Ltd., China.

Fabrication of MCC-SiO_2 heterostructures

The entire process included the process of swelling MCC with a urea solution, followed by a sol-gel process using TEOS as a precursor. Briefly, MCC was swollen with an 8 wt% urea solution for a certain time at room temperature and then leached. The swollen MCC was washed with ethanol 3 times to remove the urea solution that was not absorbed firmly by MCC and control the thickness of the adsorption layer. The treated MCC was leached and dispersed again in ethanol and then added dropwise to TEOS ethanol solution by a separating funnel. After reacting at 60 °C for 6 h, 8 mL $NH_3 \cdot H_2O$ was added to adjust the pH to 8~9, and then the solution was continually reacted for another 1 h. MCC-SiO_2 heterostructures were obtained after drying at 80 °C in a vacuum oven for 6 h. The entire process is shown in Figure 1.

Preparation of tire tread compounds

The elastomers and other ingredients, as listed in Table 1, were mixed in a torque rheometer (Rheomix 3000OS, Haake, Germany) according to the ASTM D3182-07 standard. The feeding order and mixing time of the ingredients were as follows: rubber (2 min), half of the total silica (with half of Si-69, 2 min), the other half of the silica (with remaining Si-69, 2 min) and MCC or MCC-SiO_2 (2 min), and the rest of the components (ZnO, SA, NS, DPG, 4020 and RD, 4 min). The onset temperature of the mixer was 90 °C, with a rotor speed of 70 rev/min. The sulfur was added into an open mill, and sheets with an approximate thickness of 2 mm were obtained.

A rheometer vulcanization machine (MDR-

2000, Alpha, USA) was used to measure the curing time (t_{90}) at 160 °C. The oscillating frequency was 1.7 ± 0.1 Hz, with an amplitude of ± 3.0°. The vulcanization was carried out at t_{90} in a hydraulic press (HS100T-RTMO, Shenzhen Jiaxin Co. Ltd., China) at 160 °C, and then the vulcanizates were obtained.

Table 1
Recipes of the tire tread compounds

Ingredients	Control (phr)	MCC-SiO_2 (phr)
ESBR1502	24.00	24.00
SSBR2557A	104.50	104.50
1165MP	60.00	60.00
MCC	10.00	0
MCC-SiO_2	0	10.00
SA	2.00	
ZnO	3.00	
Si69	5.60	
Antioxidant 4020	2.50	
Antioxidant RD	1.50	
Wax	1.00	
DPG	1.00	
TBBS (NS)	1.80	
Sulfur	1.60	

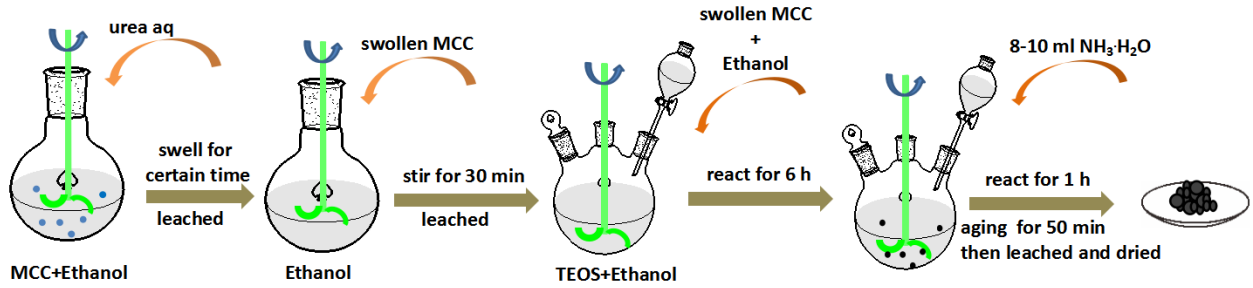

Figure 1: Fabrication processes for MCC-SiO_2 heterostructures (samples named as MS-x-y according to their preparation conditions: MS stands for MCC-SiO_2 heterostructures, x – swelling time (12 h, 24 h or 36 h), and y – TEOS usage (20 g, 15 g, 10 g or 5 g)

Characterization of MCC heterostructures

Fourier transform infrared spectroscopy (FT-IR)

MCC and MCC heterostructures were ground and tableted with KBr powder and then tested using a Fourier infrared transform spectrometer (VERTEX70, Bruker Corporation, Germany) with scanning wavenumbers ranging between 400-4000 cm^{-1}.

Thermogravimetric analysis (TGA)

A NETZSCH thermogravimetric analyzer (209F1, NETZSCH, Germany) was used to study the mass loss of MCC and MCC-SiO_2 heterostructures when heated from 30 to 800 °C, with a heating rate of 20 °C/min. The test was conducted in a nitrogen atmosphere with a flow rate of 50 mL/min.

Wide-angle X-ray diffractometry (WARD)

The XRD spectra of the MCC, swollen MCC and MCC-SiO_2 heterostructures were obtained with a wide-angle X-ray diffractometer (Ultima IV, Rigaku, Japan), with a Cu Kα source at 40 kV and 40 mA.

Field-emission scanning electron microscopy (SEM)

The microstructures of the MCC and MCC-SiO_2 heterostructures were investigated by a field-emission scanning electron microscope (JSM-

7500F, JEOL Ltd., Japan). All the samples were sputtered with a layer of platinum before SEM scanning measurements.

Characterization of rubber compounds

Mechanical properties of vulcanizates

An electron tensile testing machine (TUM 1445, Zwick, Germany) was used to measure the physical and mechanical properties of the vulcanizates, including the tensile strength (ASTM D412), the moduli at 100% and 300% elongation (ASTM D412) and the tear strength (ASTM D624). The resilience (ASTM D2632) and shore hardness (ASTM D2240) were investigated according to their respective ASTM standards.

Abrasion resistance

A DIN abrader (GT-7012-D, Gotech Testing Machines Co Ltd., Taiwan) was used to measure the DIN abrasion resistance of the vulcanizates following ASTM D5963. A cylindrical rubber specimen with a diameter of 16 mm and a height of 10 mm was abraded against a rotating cylindrical drum (150 mm in diameter, rotating at approximately 40 rev/min). The specimen was gripped in a steel collet chuck and was clamped tightly into the specimen holder, with a portion of the specimen protruding 2 mm from the clamping aperture with a gauge. The chuck moved at approximately 3 mm/s when the drum rotated at approximately 40 rev/min, and the chuck was parallel to the axis of the drum. After the specimen slid for 120 s, the total loss was tested, and the loss volume of the sample was measured combined with its density.

Dynamic mechanical analysis (DMA)

The dynamic mechanical properties of the vulcanizates were tested by a dynamic mechanical analyzer (EPLEXOR 500N, GABO, Germany) at a constant frequency of 10 Hz. The temperature ranged from -80 to 80 °C, with a heating rate of 3 °C/min. The specimens were 20 mm in length, 4 mm in width and 2 mm in thickness. The loss angle tangent (tanδ) was measured as a function of temperature under identical conditions.

Compression heat build-up

The compression heat build-up measurements were carried out in a flexometer (GT-RH2000, Gotech Testing Machines Inc., China) according to ASTM D623. A cylindrical rubber specimen with a height of 25 mm and a diameter of 17.5 mm was subjected to repeated compression with a frequency of 30 Hz. The compressive loading was 24.5 kilograms, and the onset temperature was 55 ± 1 °C. The internal temperature of the rubber composites was recorded after 25 min. Three specimens were measured for each sample, and the average values were calculated.

SEM analysis

The vulcanizates were stretched to fracture at room temperature, and the section morphology was observed by SEM. The section was sprayed with a thin layer of platinum before observation.

RESULTS AND DISCUSSION

Characterization of MCC-SiO_2 heterostructures

Structure of MCC-SiO_2 heterostructures

Figure 2 (a) shows the FT-IR spectra of the MCC and MCC-SiO_2 heterostructures. The peaks at 810 cm^{-1} and 456 cm^{-1} for the MCC-SiO_2 sample were caused by the stretching vibration and the deformation vibration of Si-O bonds, respectively, associated with the inorganic Si-O-Si network.[27] In addition, the stretching vibration of Si-O-Si at 1109 cm^{-1} resulted in a large peak at 1000-1200 cm^{-1}. These results indicated that SiO_2 was successfully loaded on the MCC surface. It is well known that the hydroxyl stretching vibration peak shifts to a lower wavenumber and that the deformation vibration peak shifts to a higher wavenumber if intermolecular hydrogen bonds exist.[28,29] The band at 3357.9 cm^{-1} was associated with the stretching vibration of the hydroxyl groups (-OH) in the IR spectrum of the MCC, whereas this peak was enhanced and shifted to a lower wavenumber of 3346 cm^{-1} for the MCC-SiO_2 sample. Furthermore, the band at 1056.9 cm^{-1} for MCC, attributed to O-H deformation vibration, was enhanced and shifted to 1060.8 cm^{-1} for the MCC-SiO_2 samples, indicating a strong hydrogen interaction between MCC and SiO_2.

Figure 2 (b) shows the XRD spectra of the MCC, MCC swollen by NaOH, MCC swollen by urea and MCC-SiO_2 (MS-36-15). The XRD spectrum of MCC showed four characteristic peaks: 22.8° (020), 34.6° (004), 14.8° ($1\bar{1}0$) and 16.3° (110), indicating a typical cellulose I crystalline structure.[30,31] However, the MCC swollen by NaOH exhibited a cellulose II crystalline form, with peaks at 2θ = 14.8°, 20.4° and 22.5°, meaning that most of the cellulose I had transformed into cellulose II. This crystal transformation harms the strength of MCC. Fortunately, the crystal form of the MCC swollen by urea, as well as that of MCC-SiO_2, had not been changed. The crystallinity was calculated by the Segal equation: $C_\gamma I = (I_{002}-I_{am})/I_{002}*100\%$, where $C_\gamma I$, I_{002} and I_{am} represent the percentage of relative

crystallinity, the maximum intensity of the lattice diffractive angle and the scattering intensity of the amorphous diffraction, respectively; these scattering intensities are located at 2θ values of approximately 22.6° and 18°, respectively. The calculated crystallinity was 84.8% for MCC, 88.58% for urea-swollen MCC, 87.48% for MCC-SiO_2 (MS-12-5), and only 66.41% for NaOH-swollen MCC. The improvement in the crystallinity of the urea-swollen MCC and MCC-SiO_2 was due to the special swelling mechanism of urea. The urea aqueous solution removed the noncrystal zone, but did not damage the crystalline region. The crystallinity of MCC-SiO_2 decreased slightly compared with that of the MCC swollen by urea because the orderly alignment of MCC molecular chains were disturbed by the strong hydrogen bond interaction between nano-SiO_2 and MCC.[32]

SiO_2 contents in heterostructures

The TGA curves of MCC-SiO_2 prepared under different conditions were compared with that of raw MCC to determine the thermostability and the number of loaded SiO_2 particles, as shown in Figure 3.

The thermal decomposition temperature of MCC was approximately 350 °C, and the residue tended to zero beyond 400 °C, indicating a complete thermal decomposition of MCC. The thermal decomposition temperature of the MCC-SiO_2 samples was lower than that of MCC because of the remaining $NH_3 \cdot H_2O$ in MCC-SiO_2, a catalyst for the thermal decomposition of MCC.

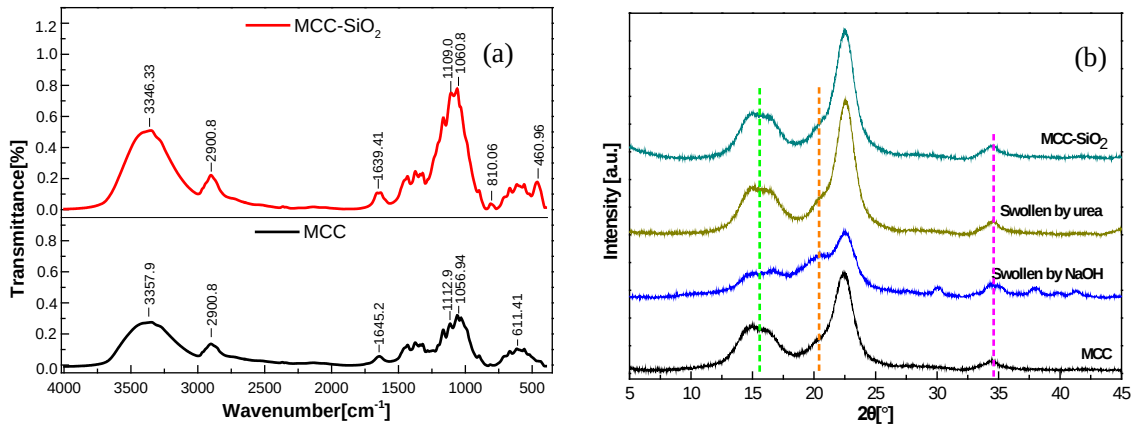

Figure 2: FT-IR (a) and XRD (b) spectra of MCC and MCC-SiO_2

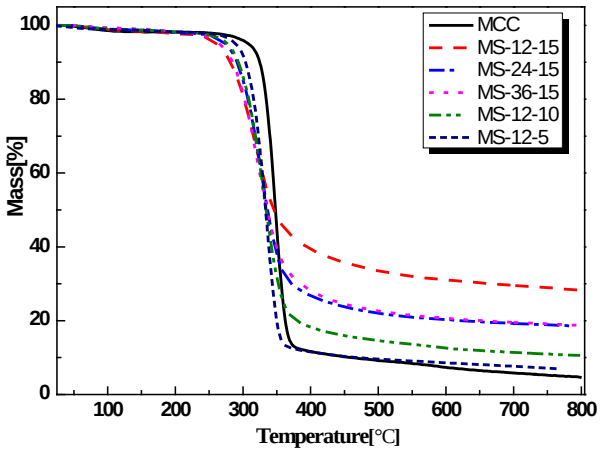

Figure 3: TGA curves of MCC and MCC-SiO_2 heterostructures

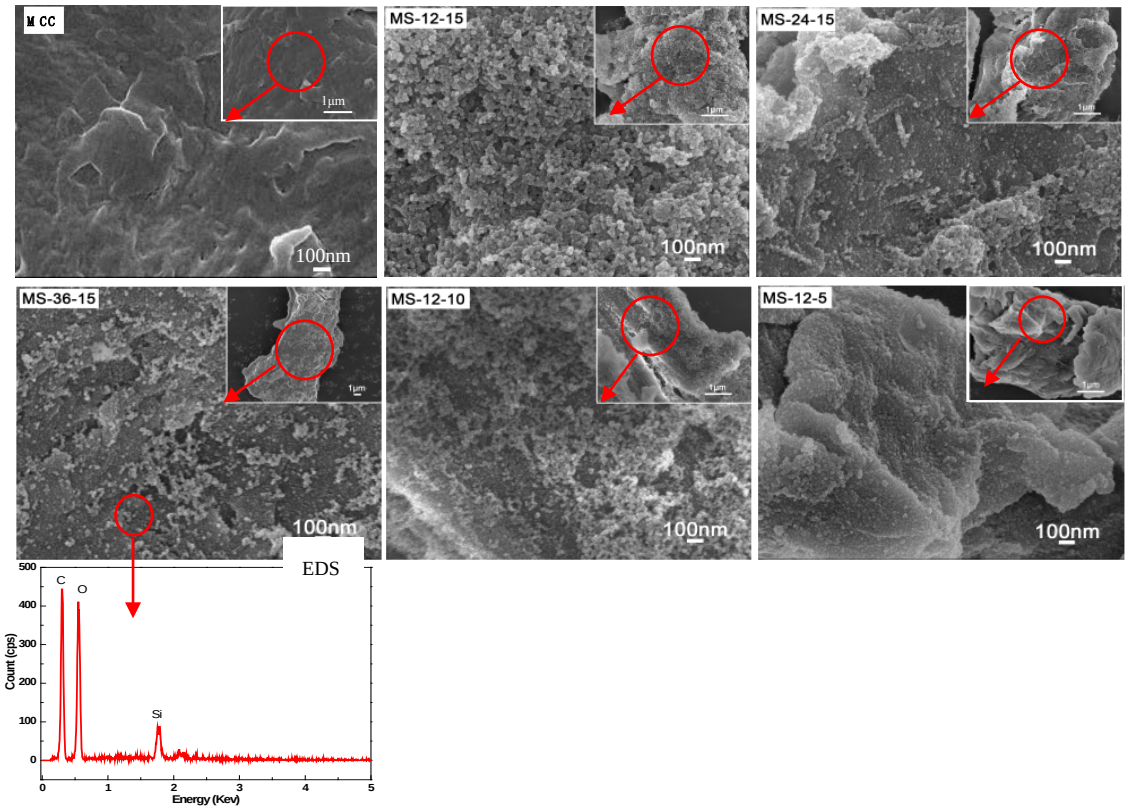

Figure 4: SEM images and EDS of MCC and MCC-SiO_2 heterostructures (the insets show low-magnification SEM images with a scale bar of 1 μm)

The residue of the MCC-SiO_2 samples was very different as the swelling time and TEOS concentration changed. The amount of SiO_2 loaded on MCC increased with increasing TEOS concentration, but decreased with increasing swelling time. It was clear that the SiO_2 load increased with increasing TEOS concentration, but it was difficult to establish that the maximum load of SiO_2 was present in the sample with minimum swelling time. The urea did not have enough time to reach and interact with the molecular chains of MCC when the swelling time was 12 h, which resulted in a higher concentration of urea in the absorbed layer of MCC and thus more SiO_2 particles generated in this layer.

Micromorphologies of MCC-SiO_2 heterostructures

The morphologies of the MCC and MCC heterostructures were observed by SEM after drying at 80 °C in a vacuum oven, and SEM and EDS photographs are shown in Figure 4.

It was found that the surface of MCC was smooth, while the surfaces of the heterostructures became rough due to the loading of SiO_2 particles. The EDS maps of part of the surface of MS-36-15 in Figure 4 confirmed that SiO_2 particles were formed. The loaded SiO_2 particles were almost spherical, with a size of 20-30 nm for samples MS-24-15, MS-36-15 and MS-12-5, and 30-40 nm for samples MS-12-15 and MS-12-10. Many aggregates overlapped on the surface of MS-12-15, and only a few aggregates overlapped on the surface of MS-12-10, while the aggregates were almost invisible on MS-24-15, MS-36-15 and MS-12-5. These results indicated that either decreasing TEOS concentration or extending swelling time decreased the number of aggregates and the particle sizes, sharing a similar regularity with the TGA results. Based on the TGA and SEM results, it was expected that MS-24-15, MS-36-15 and MS-12-5 will demonstrate better performance when used in rubber composites.

Effects of MCC-SiO_2 heterostructures on the properties of tire tread compounds

The effects of MCC (used as received) and the MCC-SiO_2 heterostructures on the physico-mechanical and dynamic mechanical

properties, as well as abrasion resistance of the vulcanizates were studied.

Physico-mechanical properties

The physical and mechanical properties of the tire tread compounds are shown in Table 2. The sample filled with MCC was used as a control. Compared with the control, the tensile strength, tear strength and elongation at break of the MCC-SiO_2 compounds were all improved, in particular, those of MS-36-15, MS-12-10, and MS-12-5. The tensile strength and elongation at break of MS-12-5 were improved by 19.3% and 18.8%, respectively, and the tear strength of MS-12-10 was improved by 16.2%. These results confirmed that the MCC-SiO_2 heterostructures had higher reinforcing efficiency than MCC alone. The improvement in the reinforcing efficiency could be attributed to the hybridization effect of nanosized SiO_2 particles with microsized MCC. As shown in the SEM images of Figure 4, the samples with regular spherical SiO_2 particles and few aggregates had much improved reinforcing efficiency. The large aggregates on MS-12-15 and MS-24-15 easily fell from the surface under the force field of rubber processing, which deteriorated the reinforcing efficiency in the rubber compounds.

"Magic triangle" of tire tread compounds

The wet-skid resistance, rolling resistance and abrasion resistance are three important features of a tire. The wet-skid resistance represents the safety of the tire, the rolling resistance represents the fuel savings, and the abrasion resistance represents the serving life. These three properties are well known as the "magic triangle" problem in the rubber industry because they are difficult to improve simultaneously.

The wet-skid resistance and rolling resistance are related to the viscoelastic properties of the rubber compounds and can be characterized by DMA (tanδ-T curves), as shown in Figure 5 (a). The tire tread compounds are expected to have a high tanδ value at 0 °C to ensure a high wet-skid resistance and a low tanδ value at 60 °C to ensure a low rolling resistance. Figure 5 (a) shows that the tanδ values of the MCC-SiO_2 (MS-24-15, MS-36-15) samples at 0 °C were significantly improved, with an approximately 52% improvement and a slight decrease at 60 °C. These results indicated that if MCC-SiO_2 was used in tire tread compounds, a much higher wet-skid resistance would be achieved, accompanied by a lower rolling resistance. In addition, the transition temperature (Tg) of the MCC-SiO_2 vulcanizates shifted to higher temperature compared with the control, indicating that MCC-SiO_2 had a strong interaction with the rubber matrix.

Figure 5 (b) shows the curves of storage modulus (E') *vs.* temperature (T) obtained from DMA data. It is clear that the storage modulus of MCC-SiO_2 compounds was much lower than that of the MCC compounds at low temperature (< -20 °C). A low storage modulus is helpful to the safety of the tire when rolling on ice and snow roads.

Figure 5 (c) shows the DIN abrasion resistance of the tire tread compounds. The abrasion loss of all the MCC-SiO_2 samples was much lower than that of the control, meaning that the MCC-SiO_2 significantly improved the abrasion resistance, especially those of MS-12-10 and MS-12-15. The significant improvement in the DIN abrasion resistance of MS-12-10 and MS-12-15 was attributed to the improvement in the high tensile strength and resilience of the vulcanizates.

Table 2
Effects of MCC-SiO_2 on the mechanical properties of the vulcanizates

Properties	Control	MS-12-15	MS-24-15	MS-36-15	MS-12-10	MS-12-5
Tensile strength, MPa	15.0	15.4	16.8	17.5	17.5	17.9
Elongation at break, %	437	487	479	491	483	519
Tear strength, $kN.m^{-1}$	45.7	48.2	50.6	51.1	53.1	52.3
300% modulus, MPa	9.94	8.63	9.46	9.68	9.24	9.67
Resilience, %	21	20	20	20	24	25
Hardness/Shore A	67	67	67	68	67	68

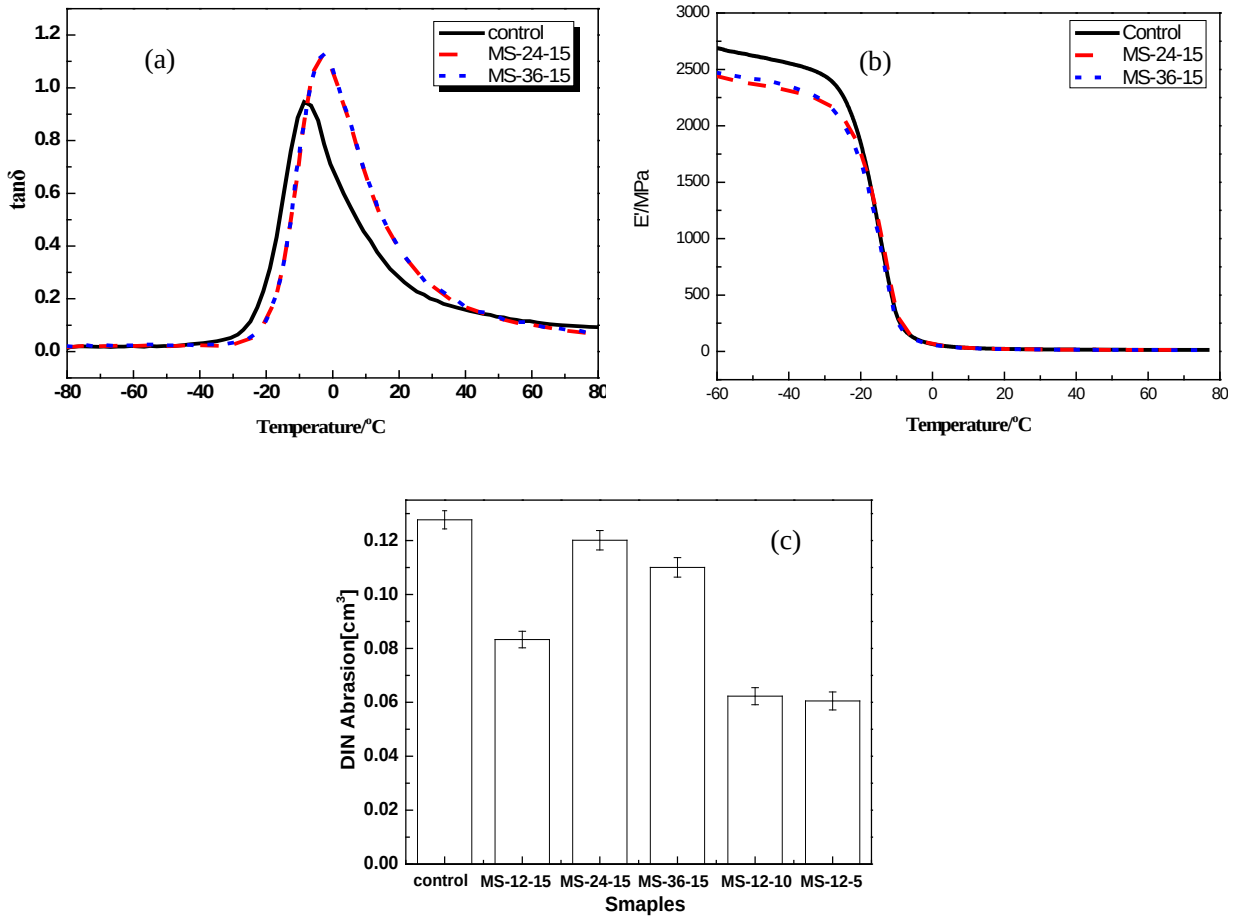

Figure 5: "Magic triangle" of tire tread compounds: (a) tanδ-T curves, (b) E'-T curves, (c) DIN abrasion resistance

Fracture morphologies of vulcanizates

The failure surfaces of the tensile samples were observed by SEM to study the microstructure and dispersion of MCC and MCC-SiO_2 in the rubber matrix, and the photographs are shown in Figure 6. The raw MCC particles, with a size of approximately 20-90 μm, had poor interface bonding with the rubber matrix, as observed in Figure 6 (a). Most of the MCC particles were pulled out of the rubber matrix, leaving many large holes in the matrix. The stress concentration often appeared in the crack tip and caused damage and failure of the material, which was the main reason for the inferior reinforcing efficiency of MCC. Compared to the raw MCC, the MCC-SiO_2 particles exhibited improved interface bonding with the rubber matrix, as shown in Figure 6 (b, c). Almost no MCC-SiO_2 particles were pulled out, and no separated interface existed, showing strong interaction between the MCC-SiO_2 particles and the rubber matrix. In addition, Figure 6 (d) shows that the MCC-SiO_2 heterostructures were maintained in the vulcanizates, indicating that nano-SiO_2 particles on the MCC-SiO_2 surfaces had not been peeled off under the stress field during the rubber processing. In addition to strong interface bonding with the rubber matrix, the sizes of the MCC-SiO_2 heterostructures were approximately 1-10 μm, as shown in Figure 6 (b), much smaller than those of the MCC particles. The MCC-SiO_2 heterostructures were disintegrated into small particles *in situ* under the strong force field during rubber processing due to the loose structure of swollen MCC.[24] Due to the *in situ* micronization and the improved interaction with the rubber matrix, the MCC-SiO_2 heterostructures had perfect reinforcing efficiency.

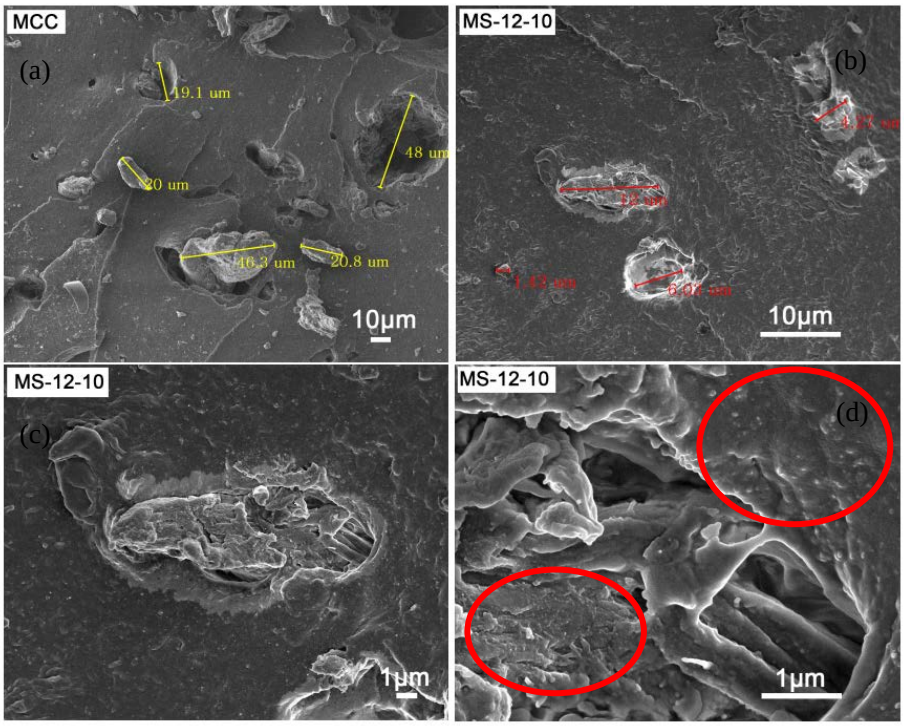

Figure 6: SEM images of fracture morphology of the tire tread compounds

CONCLUSION

MCC-SiO_2 heterostructures were achieved by loading spherical nano-SiO_2 particles on the surface of MCC through APRT combined with sol-gel technology. The aggregation states and sizes of the nano-SiO_2 particles were controllable by changing the MCC swelling time and the TEOS concentration. Decreasing the TEOS concentration and extending the swelling time both decreased the number of aggregates and the particle sizes of SiO_2, resulting in an improvement in their reinforcing efficiency in the rubber compounds. The vulcanizates filled with MS-36-15 or MS-12-10 had improved tensile strength and tear strength, and especially, improved DIN abrasion resistance. Furthermore, the wet-skid resistance (0 °C tanδ) was significantly improved as the rolling resistance (60 °C tanδ) decreased. These results indicated that MCC-SiO_2 heterostructures have great potential to solve the “magic triangle” problem in “green tire” tread compounds. SEM images showed that, compared with raw MCC, the MCC-SiO_2 heterostructures were micronized *in situ* and had improved interfacial bonding with the rubber matrix.

ACKNOWLEDGMENTS: The authors acknowledge the financial support from the Key Research and Development Project of Shandong Province (2018GSF117019) and the Key Laboratory of Rubber-Plastics, Ministry of Education/Shandong Provincial Key Laboratory of Rubber-Plastics (KF201704).

Conflict of interest: The authors declare that they have no conflict of interest.

REFERENCES

[1] S. Wang, A. Lu and L. Zhang, *Prog. Polym. Sci.*, **53**, 169 (2016), https://doi.org/10.1016/j.progpolymsci.2015.07.003
[2] F. Gu, W. X. Wang, Z. S. Cai, F. Xue, Y. C. Jin *et al.*, *Cellulose*, **25**, 2861 (2018), https://doi.org/10.1007/s10570-018-1765-8
[3] H. Wang, G. Gurau and R. D. Rogers, *Chem. Soc. Rev.*, **41**, 1519 (2012), https://10.1039/c2cs15311d
[4] M. A. Faris, T. H. Mohammed and F. Osama, *J. Clean. Prod.*, **241**, 118256 (2019), https://doi.org/10.1016/j.jclepro.2019.118256
[5] Y. Habibi, L. A. Lucia and O. J. Rojas, *Chem. Rev.*, **110**, 3479 (2010), https:/doi.org/10.1021/cr900339w
[6] C. Tsioptsias, A. Stefopoulos, I. Kokkinomalis, L. Papadopoulou and C. Panayiotou, *Green Chem.*, **10**, 965 (2008), https://doi.org/0.1039/b803869d
[7] G. Chinga-Carrasco and K. Syverud, *J.*

Nanopart. Res., **12**, 841 (2009), https://doi.org/10.1007/s11051-009-9710-2
[8] N. Chen, G. M. Zhang, P. Y. Zhang, X. Tao, Y. Wu *et al*., *Bioresour. Technol*., **292**, 121915 (2019), https://doi.org/10.1016/j.biortech.2019.121915
[9] D. D. Qiang, M. Y. Zhang, J. B. Li, H. J. Xiu and Q. Liu, *Cellulose*, **23**, 1199 (2016), https://doi.org/10.1007/s10570-016-0858-5
[10] W. S. Hou, C. Ling, S. Shi and Z. F. Yan, *Int. J. Biol. Macromol*., **354**, 35 (2015), https://doi.org/10.1016/j.ijbiomac.2018.11.112
[11] A. S. Perlin and S. Suzuki, *Can. J. Chem*., **40**, 50 (2011), https://doi.org/10.1139/v62-009
[12] N. L. G. D. Rodriguez, W. Thielemans and A. Dufresne, *Cellulose*, **13**, 261 (2006), https://doi.org/10.1007/s10570-005-9039-7
[13] A. Bendahou, Y. Habibi, H. Kaddami and A. Dufresne, *J. Biobased Mater. Bio*., **3**, 81 (2009), https://doi.org/10.1166/jbmb.2009.1011
[14] G. O. Adebayo, A. Hassan, R. Yahya, N. A. Rahman and R. Lafia-Araga, *Polym. Bull*., **76**, 6467 (2019), https://doi.org/10.1007/s00289-019-02731-0
[15] D. N. Li, J. Zhou, X. J. Ma and J. N. Li, *Cellulose*, **26**, 8729 (2019), https://doi.org/10.1007/s10570-019-02708-2
[16] L. Chazeau, J. Y. Cavaillé, G. R. Canova and R. Dendievel, *J. Appl. Polym. Sci*., **71**, 1797 (2015), https://doi.org/10.1002/(SICI)1097-4628(19990314)71:11<1797::AID-APP9>3.0.CO;2-E
[17] N. S. Prado, I. S. V. da Silva, L. C. de Morais, D. Pasquini and H. Otaguro, *J. Polym. Environ*., **27**, 2445 (2019), https://doi.org/10.1007/s10924-019-01516-w
[18] M. Fumagalli, J. Berriot, B. de Gaudemaris, A. Veyland, J. L. Putaux *et al*., *Soft Matter*, **14**, 2638 (2018), https://doi.org/10.1039/c8sm00210j
[19] F. Deng, X. Ge, Y. Zhang, M. C. Li and U. R. Cho, *J. Appl. Polym. Sci*., **132**, 18 (2015), https://doi.org/10.1002/APP.42666
[20] D. D. Chabukswar, P. K. K. S. Heer and V. G. Gaikar, *Ind. Eng. Chem. Res*., **52**, 7316 (2013), https://doi.org/10.1021/ie303089u
[21] A. Leszczynska, P. Radzik, E. Szefer, M. Micusik, M. Omastova *et al*., *Polymer*, **11**, 866 (2019), https://doi.org/10.3390/polym11050866
[22] J. Lu, P. Askeland and L. T. Drzal, *Polymer*, **49**, 1285 (2008), https://doi.org/10.1016/j.polymer.2008.01.028
[23] L. X. Gao, X. Jiang and S. Guo, *Acta Phys.-Chim. Sin*., **30**, 1303 (2014), https://doi.org/info:doi/10.3866/PKU.WHXB201405062
[24] Y. H. Liang, X. L. Liu, L. L. Wang and J. T. Sun, *Carbohyd. Polym*., **169**, 324 (2017), https://doi.org/10.1016/j.carbpol.2017.04.022
[25] J. T. Sun, X. L. Liu, Y. H. Liang, L. L. Wang and Y. Liu, *J. Appl. Polym. Sci*., **134**, 1 (2017), https://doi.org/10.1002/app.44796
[26] J. T. Sun, X. L. Liu, L. L. Wang and X. K. Shi, *J. Sol-Gel Sci. Techn*., **85**, 213 (2018), https://doi.org/10.1007/s10971-017-4521-x
[27] R. Tian, O. Seitz, M. Li, W. W. Hu, Y. J. Chabal *et al*., *Langmuir: ACS J. Surface Colloid*., **26**, 4563 (2010), https://doi.org/10.1021/la904597c
[28] B. Singh, M. Gupta, A. Verma and O. Tyagi, *Polym. Int*., **49**, 1444 (2015), https://doi.org/10.1002/1097-0126(200011)49:11<1444::AID-PI526>3.0.CO;2-9
[29] C. M. Altaner, Y. Horikawa, J. Sugiyama and M. C. Jarvis, *Cellulose*, **21**, 3171 (2014), https://doi.org/10.1007/s10570-014-0360-x
[30] J. M. Zhang, N. Luo, X. Y. Zhang, L. L. Xu, J. Wu *et al*., *ACS Sustain. Chem. Eng*., **4**, 4417 (2016), https://doi.org/10.1021/acssuschemeng.6b01034
[31] Y. Li, G. Z. Li, Y. L. Zou, Q. J. Zhou and X. X. Lian, *Cellulose*, **21**, 301 (2014), https://doi.org/10.1007/s10570-013-0146-6
[32] H. Song and L. Zheng, *Cellulose*, **20**, 1737 (2013), https://doi.org/10.1007/s10570-013-9941-3